Pergamon

Journal of Structural Geology, Vol. 19, No. 12, pp. 1537 to 1541, 1997

0191-8141/97 $17.00 + 0.00

PII: S0191-8141(97)00065-5

Brevia

SHORT NOTE

Effect of initial fault geometry on the development of fixed-hinge, fault-propagation folds

JOHN H. SPANG

Department of Geology and Geophysics and Center for Tectonophysics, Texas A & M University, College Station, TX 77843-3115, U.S.A.

and

DAVID A. McCONNELL

Department of Geology, University of Akron, Akron, OH 44325-4101, U.S.A.

(*Received* 14 *April* 1997; *accepted in revised form* 20 *August* 1997)

Abstract—This paper describes how a model of fixed-hinge, basement-involved, fault-propagation folds may be adapted to apply to thin-skinned thrust faults to generate footwall synclines. Fixed-hinge, fault-propagation folding assumes that the fold-axial surfaces diverge upwards, fold hinges are fixed in the rock, the fault propagated through the forelimb, thickness changes occur in the forelimb and the forelimb progressively rotates with increasing displacement on the underlying fault. The original model for fixed-hinge, fault-propagation folds was developed for the case of a planar fault in basement with a tip line that was at the interface between basement and the overlying sedimentary cover rocks. The two geometries applicable to thin-skinned thrusts are for the cases where a fixed-hinge fault-propagation fold develops above an initial bedding-parallel detachment, and an initial fault ramp of constant dip which flattens down-dip into a bedding-parallel detachment. © 1997 Elsevier Science Ltd.

INTRODUCTION

Asymmetric synclines in the footwall of thrust faults have been long recognized in fold-and-thrust belts (e.g. Willis, 1893; and more recently Protzman and Mitra, 1990; Fischer *et al.*, 1992; Spang, 1995). Models of fault-related folding that attempt to account for syncline development either view them as abandoned hanging wall structures (Mitra, 1990; Suppe and Medwedeff, 1990), as formed by folding prior to faulting (Fischer *et al.*, 1992) or as a combination of detachment folding and faulting (McNaught and Mitra, 1993). Here we present an additional interpretation that suggests contemporaneous faulting and footwall folding. The model is used to suggest a possible origin for a syncline in the footwall of the Rundle Thrust in the Front Ranges of the Southern Canadian Rocky Mountains.

Several models of fault-propagation folds (e.g. Mitra, 1990; Suppe and Medwedeff, 1990) assume that fold-axial surfaces are parallel and intersect the underlying thrust fault at different locations, and that the rocks are able to migrate through fold hinges. The model described in this paper is a variation of a fault-propagation fold model presented by McConnell (1994). McConnell's model assumed that axial surfaces diverge upward, fold hinges are fixed in the rocks, and units stratigraphically above the tip line of the fault rotate and change thickness as displacement increases on the underlying fault. The original model (McConnell, 1994) considered the simple case where an initial fault with constant dip cuts basement, and the tip line of the fault is initially at the interface between basement and unfaulted sedimentary cover rocks. Kinematic model predictions were compared to basement-involved folds from the Foreland Province of the Rocky Mountains (McConnell, 1994). Two additional fault configurations are discussed below. The initial fault geometries involve a layer-parallel detachment and also produce a deformed footwall, and have applicability to thin-skinned fold-and-thrust belts.

FIXED-HINGE, FAULT-PROPAGATION FOLDING

The fault-propagation fold initiates at the tip line (Fig. 1a), where the displacement is zero. The anticlinal (A–A′) and synclinal (S–S′) axial surfaces, which remain fixed in the rock, intersect at the tip line. As displacement occurs on the fault, the beds on the forelimb between the two

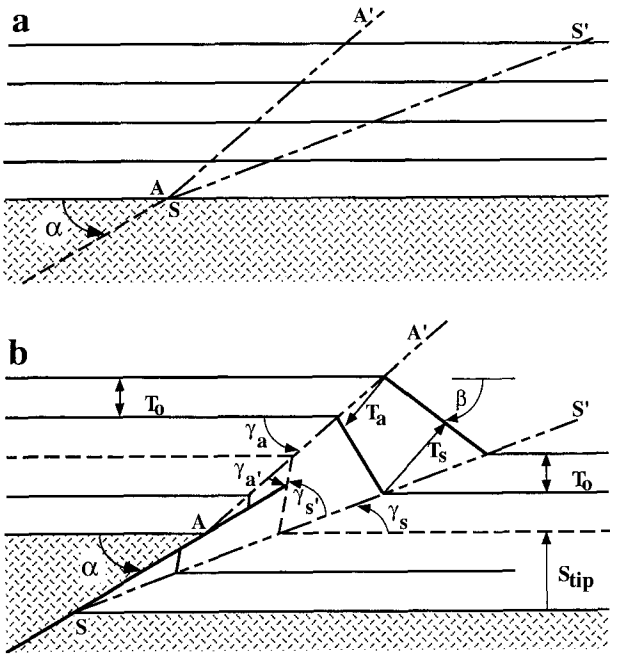

Fig. 1. Geometric elements of the kinematic model (after McConnell, 1994, fig. 4) for a fixed-hinge, fault-propagation fold. (a) The fault has a dip of $\alpha = 30°$ in this example, and the tip is at the interface between the basement (granite pattern) and the overlying sedimentary cover rocks (horizontal lines). The anticlinal axial surface (A–A′) and the synclinal axial surface (S–S′) are double-dashed lines which intersect at the fault tip. (b) T_o is the original bed thickness; S_{tip} is the stratigraphic level (dashed line) of the fault tip; β is the dip on the unfaulted forelimb; $\gamma_a + \gamma_{a'}$ is the interlimb angle for the anticline and $\gamma_s + \gamma_{s'}$ is the interlimb angle for the syncline.

axial surfaces are progressively rotated and undergo thickness changes (Fig. 1b), although their area remains constant (McConnell, 1994, p. 1586). Fault displacement decreases uniformly from a maximum at the original fault tip to zero at the new fault tip, as the fault tip propagates stratigraphically upward into the folded layers (S_{tip} in Fig. 1b). Unfaulted layers in the forelimb above the fault tip are rotated to progressively steeper dips until they are cut by the fault, after which rotation ceases. In Fig. 1(b), the rotation ceases at a value of $\gamma_{a'}$, such that $\gamma_{a'} = \gamma_a$. As these angles are equal, the resulting anticline in the hanging wall is symmetric with respect to the axial surface, and the layers on both limbs of the anticline are of equal thickness, which is also their original thickness, T_o. For the case in which the fault propagates through the layer when $\gamma_{a'} > \gamma_a$, the layers in the forelimb of the anticline would be thickened in the hanging wall (i.e. $T_a > T_o$), and in the case where $\gamma_{a'} < \gamma_a$, the layers in the forelimb would be thinned (i.e. $T_a < T_o$). Although this style of cross-section can be drawn using only simple drafting tools or a draw program on a microcomputer, all of the relationships can also be calculated using equations (see the appendix in McConnell, 1994). The trishear model for fault-propagation folding (Erslev, 1991) could also be applied to any of these initial fault geometries and would produce similar final geometries.

EFFECT OF DIFFERENT INITIAL FAULT GEOMETRIES

Figure 2 illustrates a basement-cored fold as described by McConnell (1994) and presents two modifications of that model which are applicable to faults cutting stratified rocks. Figure 2(a–c) shows the initial geometries at the onset of fault-propagation folding and uses the same geometric elements as in Fig. 1 (α, γ_a, $\gamma_{a'}$, γ_s and $\gamma_{s'}$ are the same). Figure 2(d–f) shows these initial geometries after the same amount of fault displacement. Figure 2(a & d) shows the case of a planar fault with the initial fault tip at the basement–cover rock interface (after the models of McConnell, 1994). Alternative initial fault geometries (Fig. 2b & c) make it possible to apply this method to structures other than the uplift of rigid basement blocks in the hanging wall of planar faults.

The fixed hinge model can be readily adapted to develop from an initial bedding-parallel detachment (Fig. 2b & e). This is a common geometry in thin-skinned fold-and-thrust belts, and it has frequently been used in other kinematic models (e.g. Suppe and Medwedeff, 1990; Jamison, 1987). Chester and Chester (1990) suggested that fault-propagation folds may develop above fault ramps (Fig. 2c & f) of constant dip which flatten down-dip into a horizontal detachment. In this geometry, the fixed-hinge, fault-propagation fold initiates at the tip of the dipping ramp. At the bend where the fault flattens, a fault-bend fold develops. The resulting structure (Fig. 2f) is thus a combination of fault-bend and fault-propagation folds.

The final geometry of the foreland anticline–syncline pair is exactly the same in all of the final kinematic models (Fig. 2d–f). No other fold is created when the fault is planar with constant dip (Fig. 2d). When the fault flattens (Fig. 2e & f), hinterland-verging fault-bend folds develop. The overall shape of the structures is that of a fault-cored, box-shaped anticline. The main difference in these two final models is the width of the anticline (Fig. 2e & f). Fault-bend folds develop at the base of the footwall ramp as a flat in the hanging wall is folded to move up the footwall ramp. As Fig. 2(f) started with what is equivalent to a ramp–flat geometry, the resulting box anticline is different (i.e. broader in this case) to the one in Fig. 2(e). The two different initial starting geometries introduce the concept of a structural stratigraphy, where the initial fault ramp in Fig. 2(c) may represent brittle failure in rocks that cannot deform by fault-propagation folding. Fault propagation could initiate at the top of the ramp in Fig. 2(c) due to change in rock type to units that can undergo fault-propagation folding (Chester and Chester, 1990, p. 905).

NATURAL EXAMPLE

Figure 3 depicts a major syncline (the Mt Allan Syncline) in the footwall of the Rundle Thrust in the

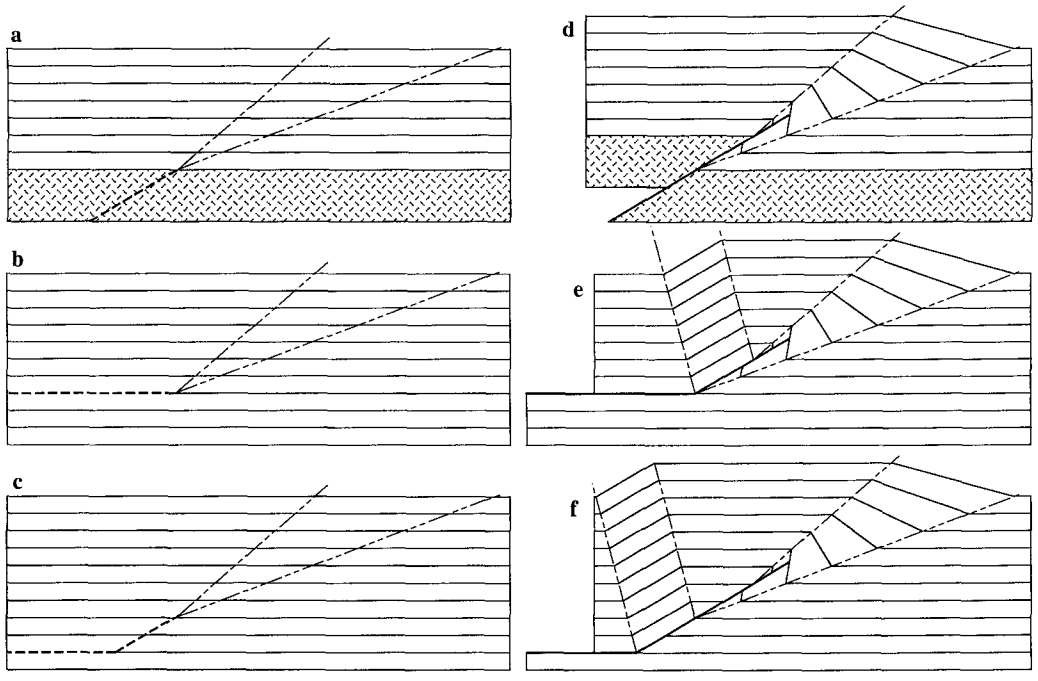

Fig. 2. Kinematic evolution of fixed-hinge, fault-propagation folds starting with different initial fault geometries. Fault-propagation folds develop above an initial (a) reverse fault (dashed line) in basement, (granite symbol) with constant dip, (b) bedding-parallel detachment, (c) ramp–flat configuration. (d), (e) and (f) represent fixed-hinge, fault-propagation folds formed after a uniform fault displacement using each of the initial geometries (a–c), and are discussed in the text.

Front Ranges of the Southern Canadian Rocky Mountains near Canmore, Alberta, Canada (redrawn from Price, 1970a,b). The syncline is locally well exposed at the surface and has relatively straight limbs with a tight curvature in the hinge region. Thickening in the hinge region is accommodated by three thrust faults, which do not appear to be related to motion on the Rundle Thrust as they do not have any Paleozoic rocks in their hanging walls. They appear to be due to motion on an earlier (structurally older and higher) thrust. Two of the thrusts

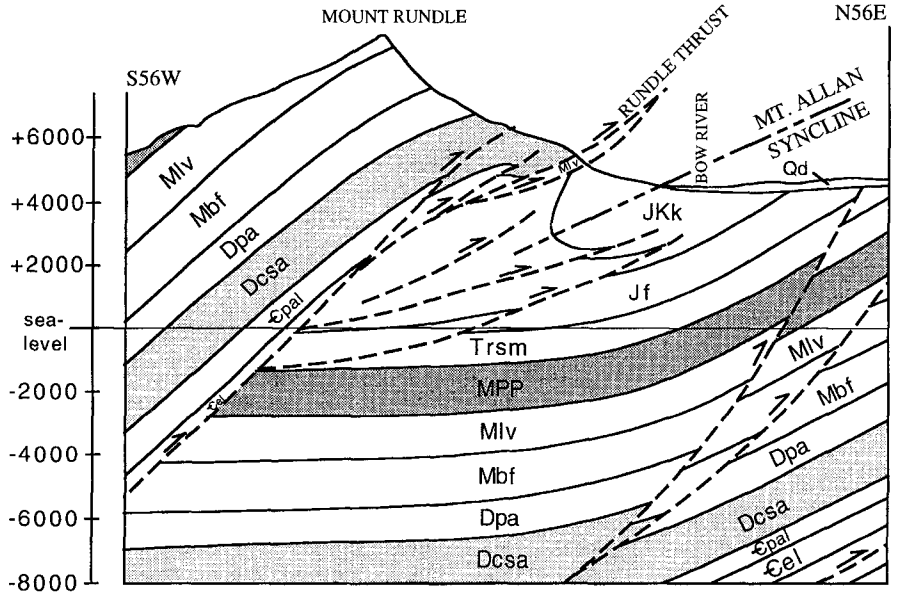

Fig. 3. A portion of a cross-section across the Rundle Thrust showing the Mt Allan Syncline in the footwall (redrawn from Price, 1970a,b). The cross-section is oriented N56°E, which is approximately parallel to the local transport direction for the Rundle Thrust (view is to the northwest). The northeastern (normal) limb of the overturned syncline has been folded due to motion on structurally lower and younger thrusts, several of which are shown on the cross-section. Cel—Eldon Formation; Cpal—Pika Formation, Arctomys Formation, Lynx Group; Dcsa—Cairn Formation, Southesk Formation, Alexo Formation; Dpa—Palliser Formation; Mbf—Banff Formation; Mlv—Livingstone Formation; MPP—Mount Head Formation, Etherington Formation, Rocky Mountain Group; Trsm—Sulphur Mountain Formation; Jf—Fernie Group; JKk—Kootenay Formation (oldest to youngest).

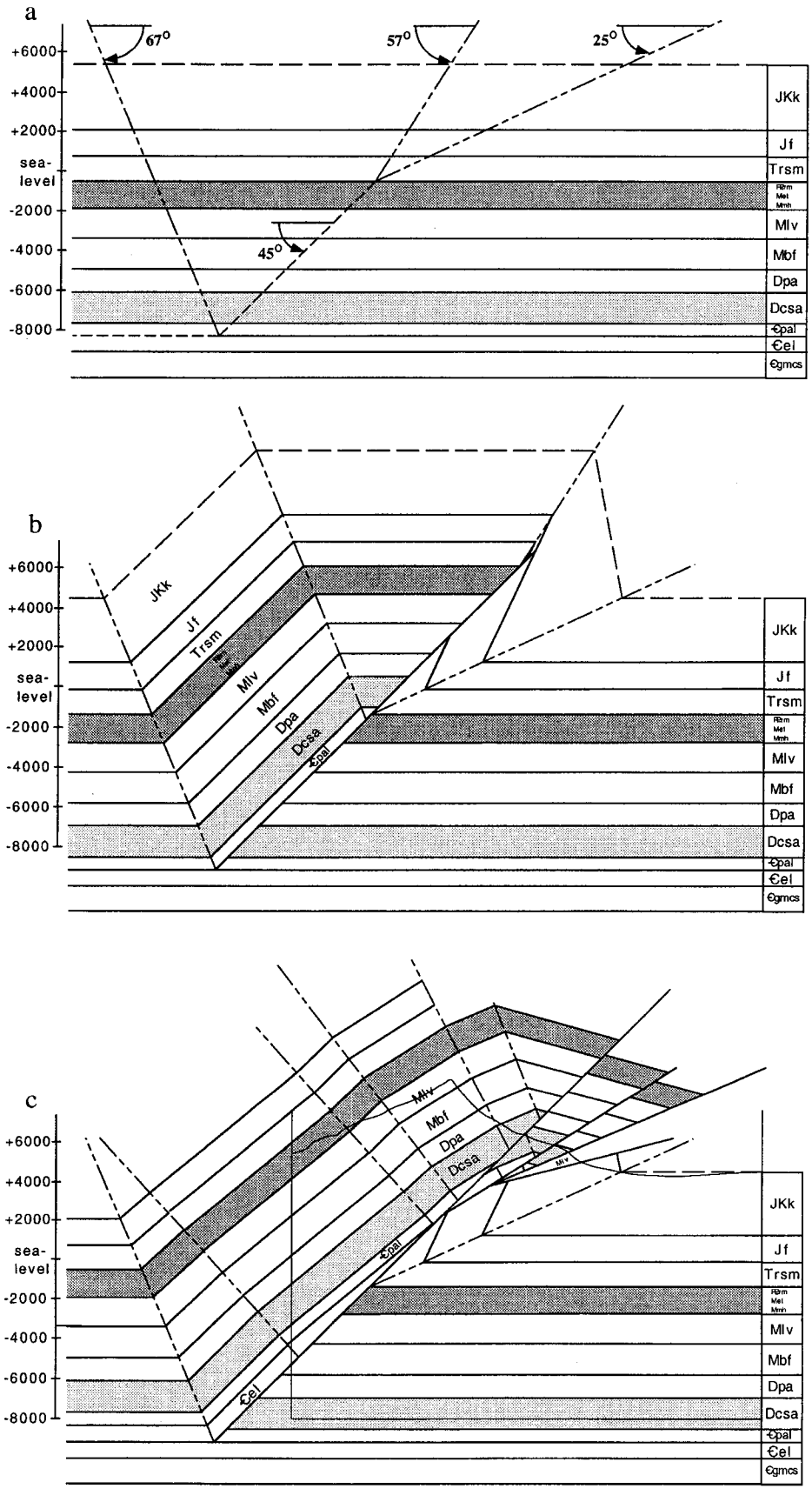

Fig. 4. Fixed-hinge, fault-propagation fold model for the cross-section in Fig. 3. (a) At zero displacement, the fault (dashed line) has a flat at the top of the Eldon Formation (Cel) and a ramp with a dip of 45° (α in Fig. 1a). Incipient axial surfaces (double dashes) for the fixed-hinge, fault-propagation fold intersect at the fault tip (A, S) and have dips of 57° (γ_a) and 25° (γ_s). The axial surface for the incipient fault-bend fold forms at the intersection of the ramp and flat, and has a dip of 67.5°. (b) Fixed-hinge, fault-propagation fold with the fault tip at the top of the Jurassic Fernie Group (Jf). (c) Hanging wall imbricates develop after the fixed-hinge, fault-propagation fold in (b) locks up.

are below the synclinal axial surface and would not be deformed by fault-propagation folding related to the Rundle Thrust. The gentle northeastern limb of the syncline has been folded by motion on structurally lower and younger thrust faults. In order to model the development of the syncline (Fig. 4), this folding has been removed.

Three possible stages in the development of this structure are shown in Fig. 4. The initial geometry (Fig. 4a) has been determined using the cut-off angle in the footwall and limb dips on the syncline measured on the original cross-section of Price (1970a,b and redrawn here as Fig. 3). In Price's section, he showed the Triassic Sulphur Mountain Formation as thickened by faulting but not by folding. Approximately 40 km southeast along strike, the Sulphur Mountain Formation is clearly part of the footwall syncline (Bielenstein, 1970), and in this same area Bielenstein has also mapped the Sulphur Mountain Formation in a syncline in the footwall of the structurally higher Lewis Thrust. If the initial geometry (Fig. 4a) is different, then the footwall syncline could extend down into the Paleozoic carbonates beneath the Sulphur Mountain Formation. Figure 4(b) shows the fault-propagation fold at some arbitrary displacement. If the fault-propagation fold had locked up at an earlier stage, the forelimb would have been rotated less at the present erosion level. When the fault-propagation fold locked up, additional shortening is interpreted to have taken place by fault-bend folding along several hanging wall imbricates to yield the final geometry shown in Fig. 4(c).

DISCUSSION

Three different initial fault geometries can be used to model thrust faults using the basic model of fixed-hinge, fault-propagation folding proposed by McConnell (1994). The beds in the forelimb of the anticline–syncline pair are continuously rotated and undergo thickness changes until they are cut by the propagating fault. Two of the models involve a layer-parallel detachment and may be most applicable to thin-skinned fold-and-thrust belts. In this model of fixed-hinge, fault-propagation folding a syncline is preserved in the footwall, and the steep limb of the footwall syncline can maintain constant thickness, thicken or thin. With the exception of the kinematic models of Erslev (1991), McConnell (1994) and Spang (1995), previous models of fault-propagation folding, fault-bend folding and detachment folding for thin-skinned thrusts typically assumed an undeformed footwall during the initial shortening (e.g. Jamison, 1987; Chester and Chester, 1990; Suppe and Medwedeff, 1990; McNaught and Mitra, 1993).

The utility of kinematic models is in their ability to reproduce the geometry of natural structures. In doing so they can provide a potential explanation for the origin of these structures. The interpretation described above offers an alternative to models that view footwall synclines as anomalous structures that are only preserved when the initial fault–fold geometry is altered. In this style of fault-propagation folding, the footwall syncline is as equally important as the hanging wall anticline, as both are formed in order to accommodate slip on the propagating thrust fault. Similarities between the kinematic model and the geological map pattern and cross-section interpretation suggest that the Mt Allan Syncline and the Rundle Thrust may have formed contemporaneously.

Acknowledgements—We benefited greatly from discussions with Dave Wiltschko, Judi Chester, Ray Price and the late Mel Friedman. Thorough reviews by Bob Ratliff, Chris Schmidt, Eric Erslev and Steve Wojtal greatly improved the manuscript.

REFERENCES

Bielenstein, H. U. (1970) The Rundle Thrust Sheet, Banff, Alberta, a structural analysis. Ph.D. thesis, Queen's University, Kingston, Ontario, Canada.

Chester, J. S. and Chester, F. M. (1990) Fault-propagation folds above thrusts with constant dip. *Journal of Structural Geology* **12**, 903–910.

Erslev, E. A. (1991) Trishear fault-propagation folding. *Geology* **19**, 617–620.

Fischer, M. P., Woodward, N. B. and Mitchell, M. M. (1992) The kinematics of break-thrust folds. *Journal of Structural Geology* **14**, 183–192.

Jamison, W. R. (1987) Geometric analysis of fold development in overthrust terrains. *Journal of Structural Geology* **9**, 207–219.

McConnell, D. A. (1994) Fixed-hinge, basement-involved fault-propagation folds, Wyoming. *Bulletin of the Geological Society of America* **106**, 1583–1593.

McNaught, M. A. and Mitra, G. (1993) A kinematic model for the origin of footwall synclines. *Journal of Structural Geology* **15**, 805–808.

Mitra, S. (1990) Fault-propagation folds: Geometry, kinematic evolution, and hydrocarbon traps. *Bulletin of the American Association of Petroleum Geologists* **74**, 921–945.

Price, R. A. (1970a) *Geology, Canmore (East Half) Alberta.* Geological Survey of Canada Map **1265A**.

Price, R. A. (1970b) *Geology, Canmore (West Half) Alberta.* Geological Survey of Canada Map **1266A**.

Protzman, G. M. and Mitra, G. (1990) Strain fabric associated with the Meade thrust sheet: implications for cross-section balancing. *Journal of Structural Geology* **12**, 403–417.

Spang, J.H. (1995) Self-similar models of fault-propagation synclines in the footwall of thrust faults. *Geological Society of America, Abstracts with Programs* **27**, A–123.

Suppe, J. and Medwedeff, D. A. (1990) Geometry and kinematics of fault-propagation folding. *Eclogae Geologicae Helvetiae* **83**, 409–454.

Willis, B. (1893) The mechanics of Appalachian structure. In *U.S. Geological Survey, 13th Annual Report, part 2*, pp. 211–281.